DYNAMICAL AND THERMAL EFFECTS OF NONLINEAR ACOUSTIC-GRAVITY WAVES IN THE UPPER ATMOSPHERE AT HIGH AND LOW SOLAR ACTIVITY.

Nikolai M. Gavrilov
Atmosphere Physics Department,
Saint-Petersburg State University, Russia

Sergey P. Kshevetskii
Theoretical Physics Department
Immanuel Kant Baltic Federal University
Kaliningrad, Russia

1. **Numerical wave model**
2. **AGW surface sources**
3. **Low and high solar activity**
4. **AGW amplitudes**
5. **Wave-induced heating and jets**
6. **AGW thermal effect**
7. **Conclusion**

Main Equations

The Equation of Continuity

$$\partial \rho / \partial t + \partial (\rho v_{\alpha}) / \partial x_{\alpha} = 0;$$

The Equations of Motion

$$\frac{\partial \rho v_i}{\partial t} + \frac{\partial \rho v_i v_{\alpha}}{\partial x_{\alpha}} = -\frac{\partial p}{\partial x_i} - \rho g \delta_{i3} + \rho X_i + \frac{\partial \sigma_{i\alpha}}{\partial x_{\alpha}}; i, \alpha = 1, 2, 3$$

The Equation of State of ideal gas

$$p = \rho R T;$$

The Heat Balance Equation

$$\frac{dp}{dt} = -\gamma p \, div \vec{v} + (\gamma - 1) \frac{dQ}{dt},$$

$$\frac{dQ}{dt} = \rho(\varepsilon_t + \varepsilon_d + \varepsilon); \quad \rho \varepsilon_d = \sigma_{\alpha\beta} \frac{\partial v_{\alpha}}{\partial x_{\beta}}; \quad \rho \varepsilon_t = -\frac{\partial q_{m\alpha}}{\partial x_{\alpha}}.$$

Molecular and Turbulent Viscosity and Heat Conduction

$$\sigma_{ij} = \mu \partial v_i / \partial x_j ,$$

$$q_i = -\kappa \partial T / \partial x_i .$$

Coefficients μ and κ take account of molecular and turbulent viscosity and heat conduction, respectively

Vertical Boundary Conditions

The upper boundary conditions at altitude h=500 km

$$\left(\frac{\partial T'}{\partial z}\right)_{z=h} = 0, \left(\frac{\partial u}{\partial z}\right)_{z=h} = 0, (w)_{z=h} = 0$$

Lower boundary conditions at the Earth surface

$$(T')_{z=0} = 0, \quad (u)_{z=0} = 0,$$

$$(\mathrm{w})_{z=0} = a \sin[\sigma(t\text{-}x/c_x)],$$

The condition for *w* at the lower boundary is a source of waves in the model.

Horizontal Boundary Conditions

Periodical conditions at horizontal boundaries

$$\alpha(x, z, t) = \alpha(x + L_x, z, t),$$

$$\alpha(y, z, t) = \alpha(y + L_y, z, t),$$

Where $L_x = n\lambda_x; L_y = m\lambda_y;$

$$\lambda_x = 2\pi / k_x; \quad \lambda_y = 2\pi / k_y;$$

are horizontal dimensions of atmospheric domain;

k_x, k_y **are horizontal wavenumbers.**

2. AGW surface sources

Plane Wave Excitation

$$w(x, y, z = 0, t) =$$

$$= W_0 \times \cos\left(\sigma \left(t - \frac{x}{c_x} - \frac{y}{c_y}\right) \right)$$

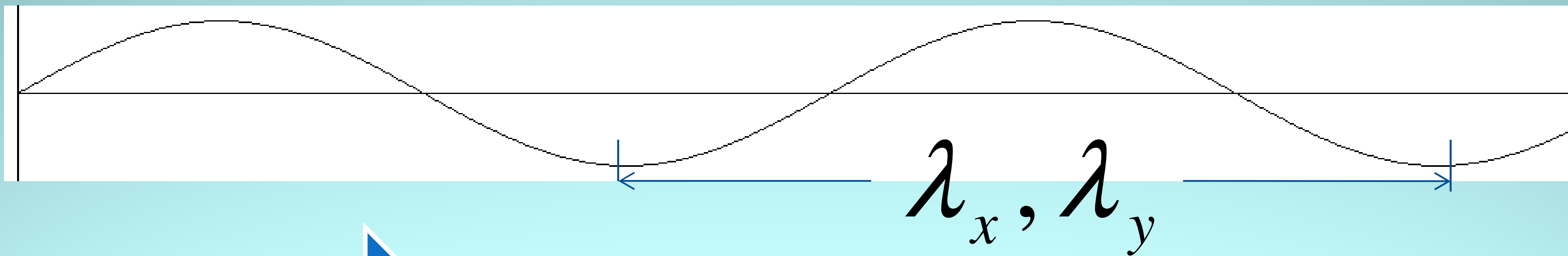

Phase velocity

$$c_i = \frac{\sigma}{k_i}; \qquad k_i = \frac{2\pi}{\lambda_i}.$$

3. Low and high solar activity

Atmospheric parameters for different solar $F_{10.7}$ radiowave flux from the NRLMSISE-00 model

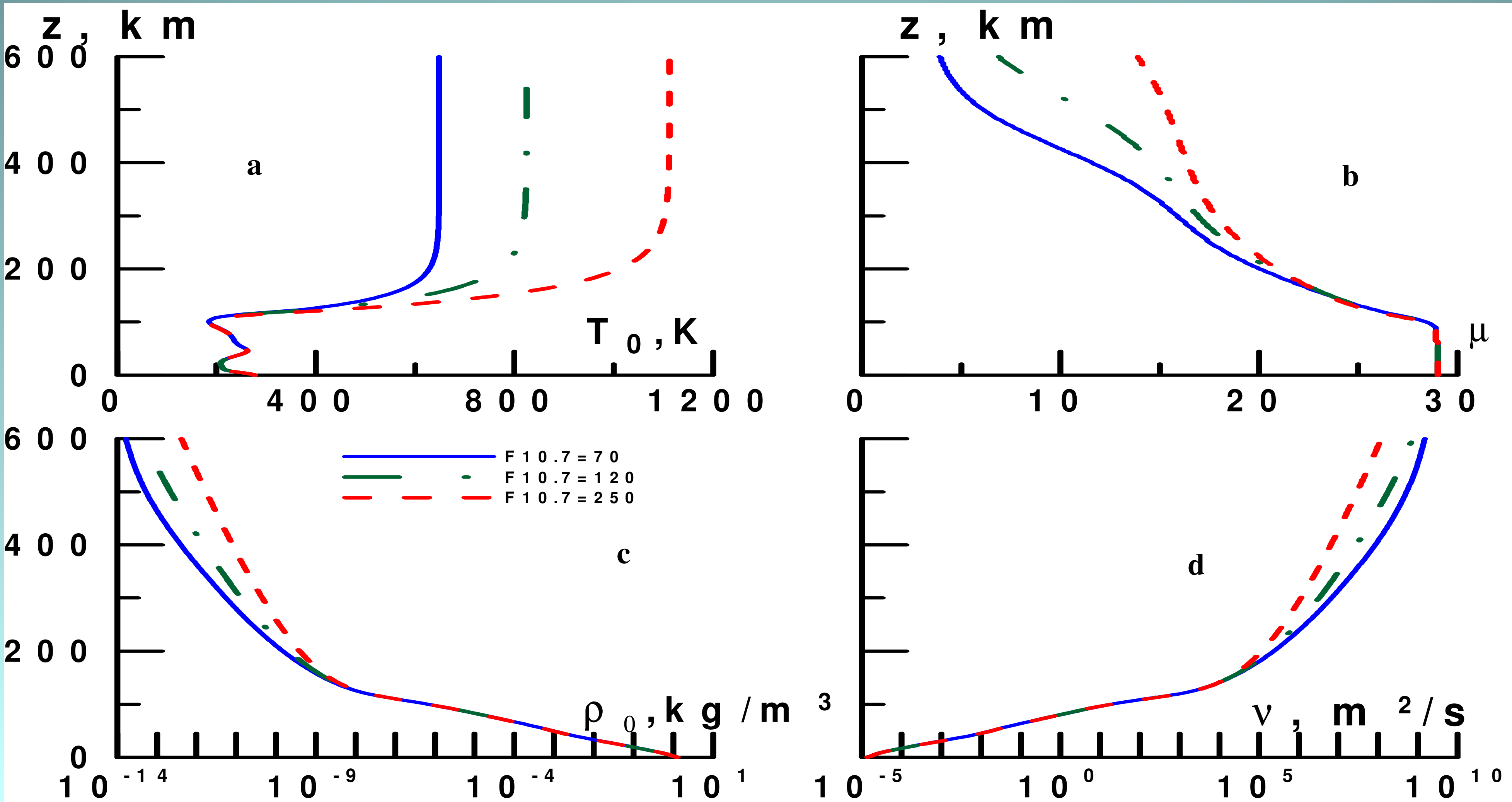

Background temperature (a), molecular weight (b), density (c) and kinematic viscosity (d)

Vertical velocity (in m/s) in the plane XOZ parallel to the horizontal wave vector at time $t = 9\tau$ for values of solar radiowave flux

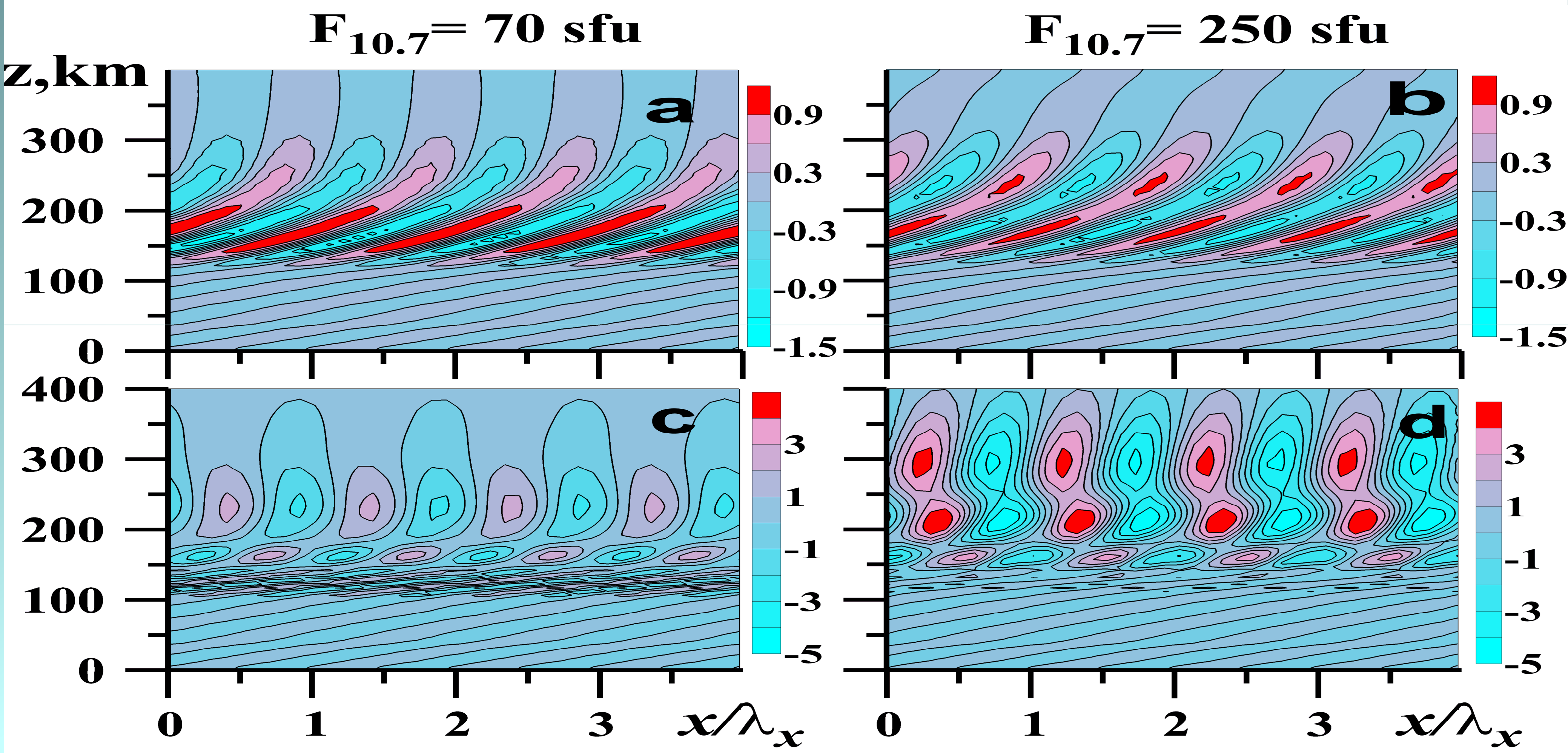

Wave source amplitudes W_0 = 0.1 mm/s (a,b) and W_0 = 1 mm/s (c,d), period $\tau = 2\times10^3$ s and c_x = 100 m/s and interval of wave activation t_0 = 1 s

4. AGW amplitudes at low and high solar activity

Vertical velocity perturbations from AGW source with period $\tau = 2\times10^3$ s and c_x = 100 m/s at time $t = 55\tau$ for different solar radiowave flux

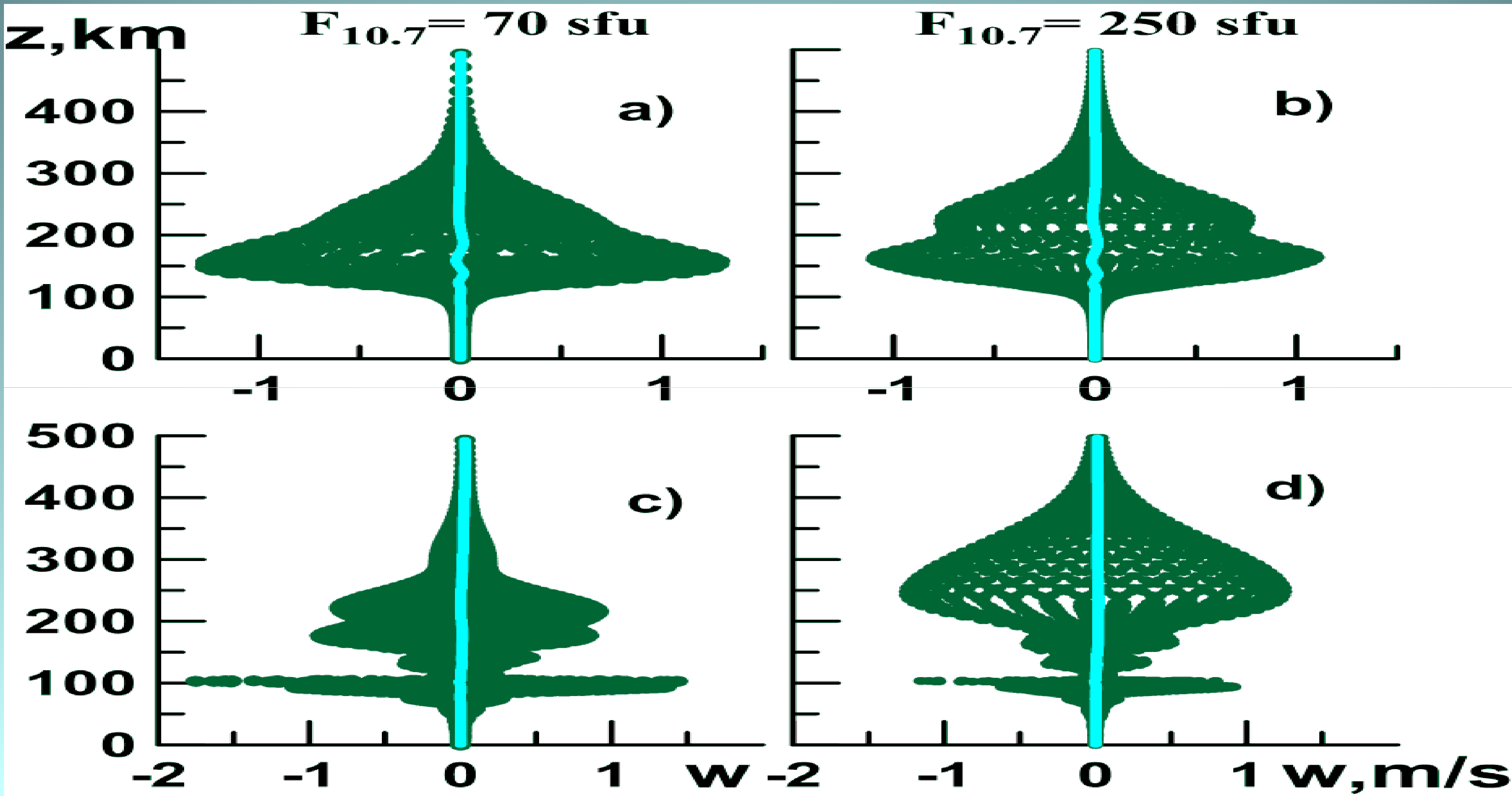

Source amplitudes W_0 = 0.1 mm/s (a,b) and W_0 = 1 mm/s (c,d).
Thick lines show average values for each altitude.

Simulated standard deviation of vertical velocity

at Z = 250 (a), 200 (b), 150 (c), 120 (d), 110 km (e) for amplitudes W_0 = 0.1 mm/s (left) and W_0 = 1 mm/s (right) of the wave forcing with period τ = $2 \cdot 10^3$ s and c_x = 100 m/s at low (blue) and high (red) levels of solar activity.

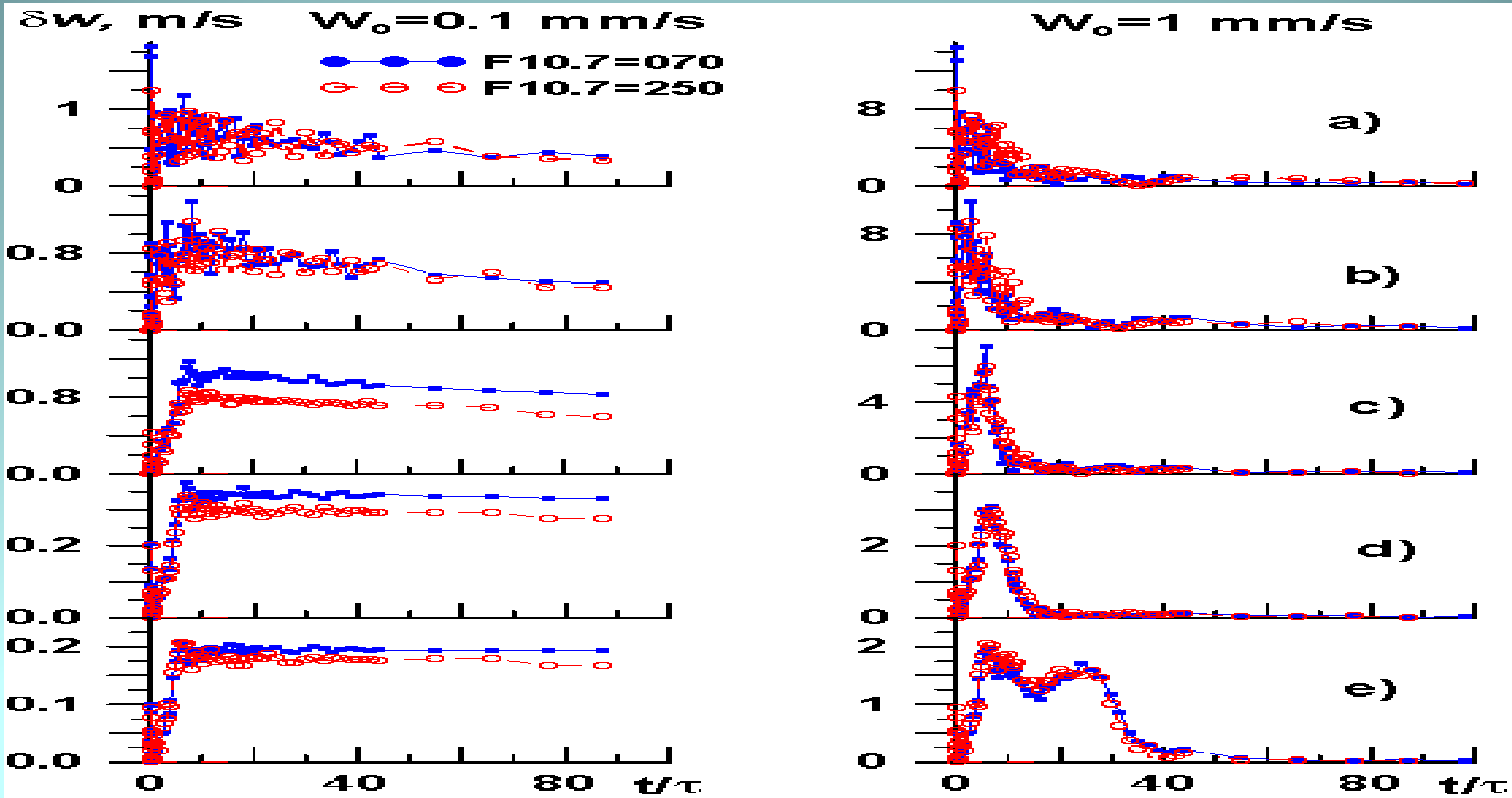

Simulated standard deviation of horizontal velocity

at Z = 250 (a), 200 (b), 150 (c), 120 (d), 110 km (e) for amplitudes W_0 = 0.1 mm/s (left) and W_0 = 1 mm/s (right) of the wave forcing with period $\tau = 2 \cdot 10^3$ s and c_x = 100 m/s at low (blue) and high (red) levels of solar activity.

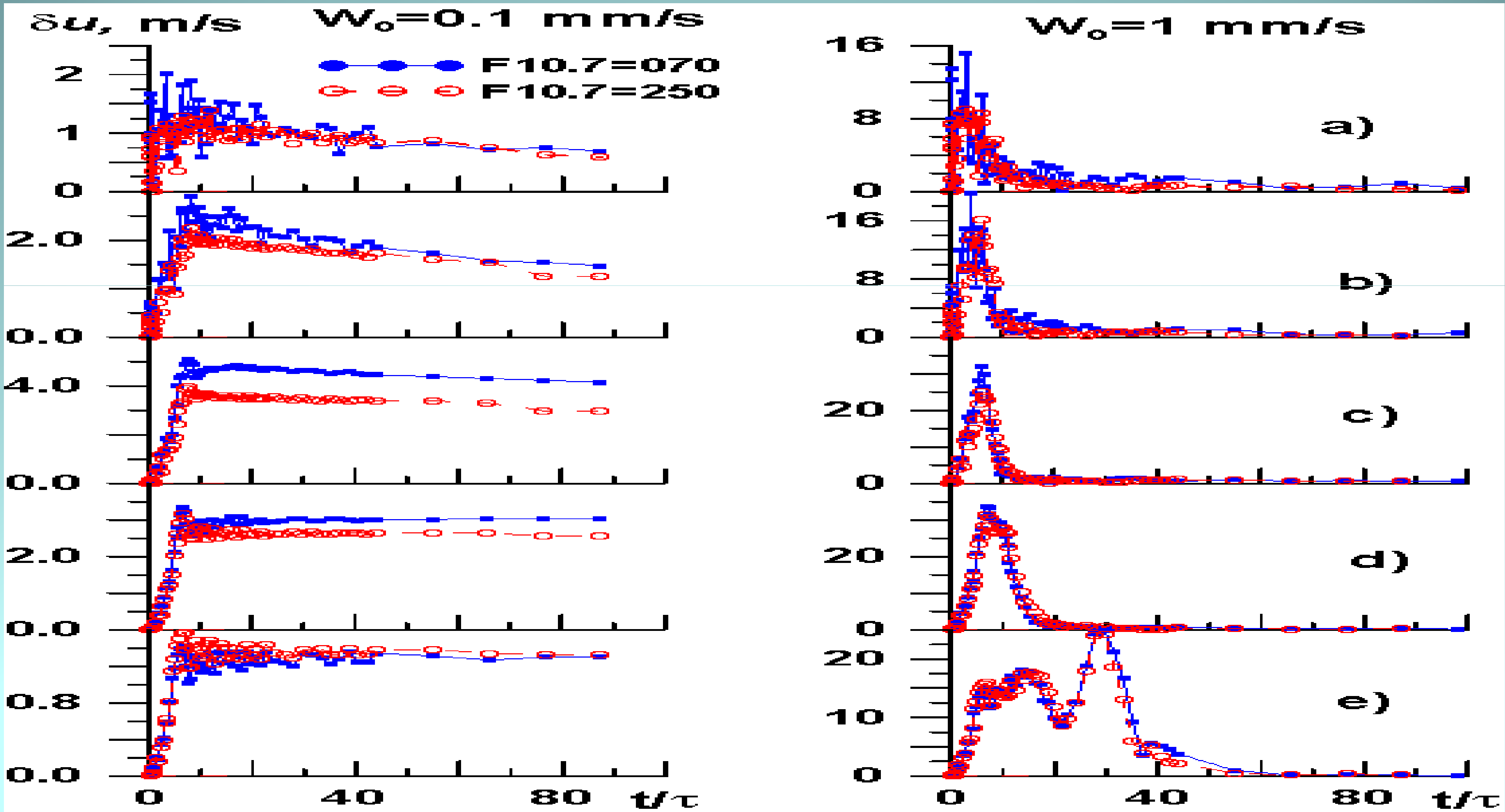

Time variations of the temperature standard deviation

at altitudes 250 (a), 200 (b), 150 (c), 120 (d), 110 km (e) for amplitudes $W_0 = 0.1$ mm/s (left) and $W_0 = 1$ mm/s (right) of the surface wave forcing with period $\tau = 2 \cdot 10^3$ s and $c_x = 100$ m/s at low (blue) and high (red) levels of solar activity.

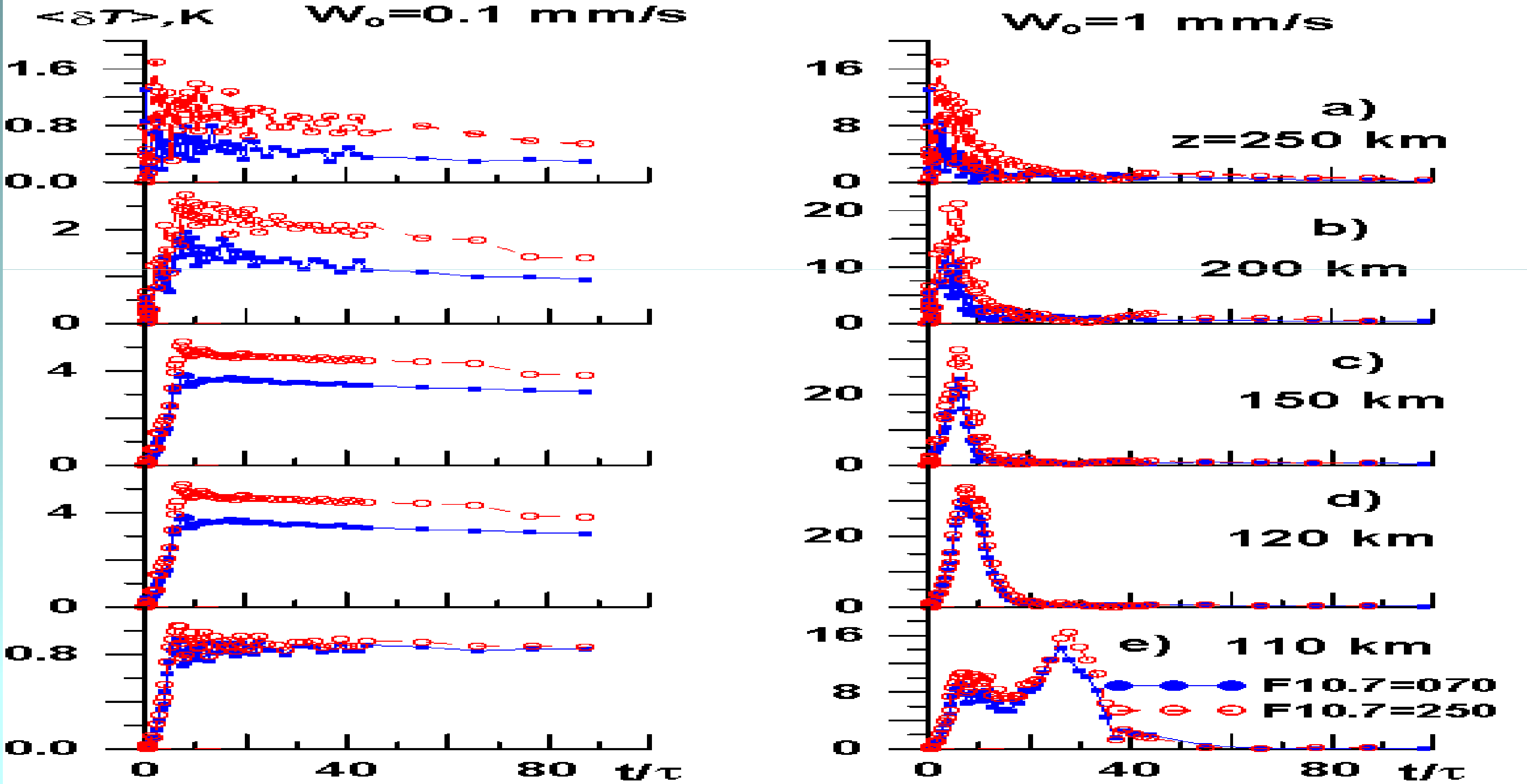

5. Wave-induced mean flows

Horizontal velocity perturbations from AGW source

with period $\tau = 2\times10^3$ s and $c_x = 100$ m/s and amplitudes $W_0 = 0.1$ mm/s (a,b) and $W_0 = 1$ mm/s (c,d) at time $t = 55\tau$ for different values of solar radiowave flux). Thick lines show average values for each altitude.

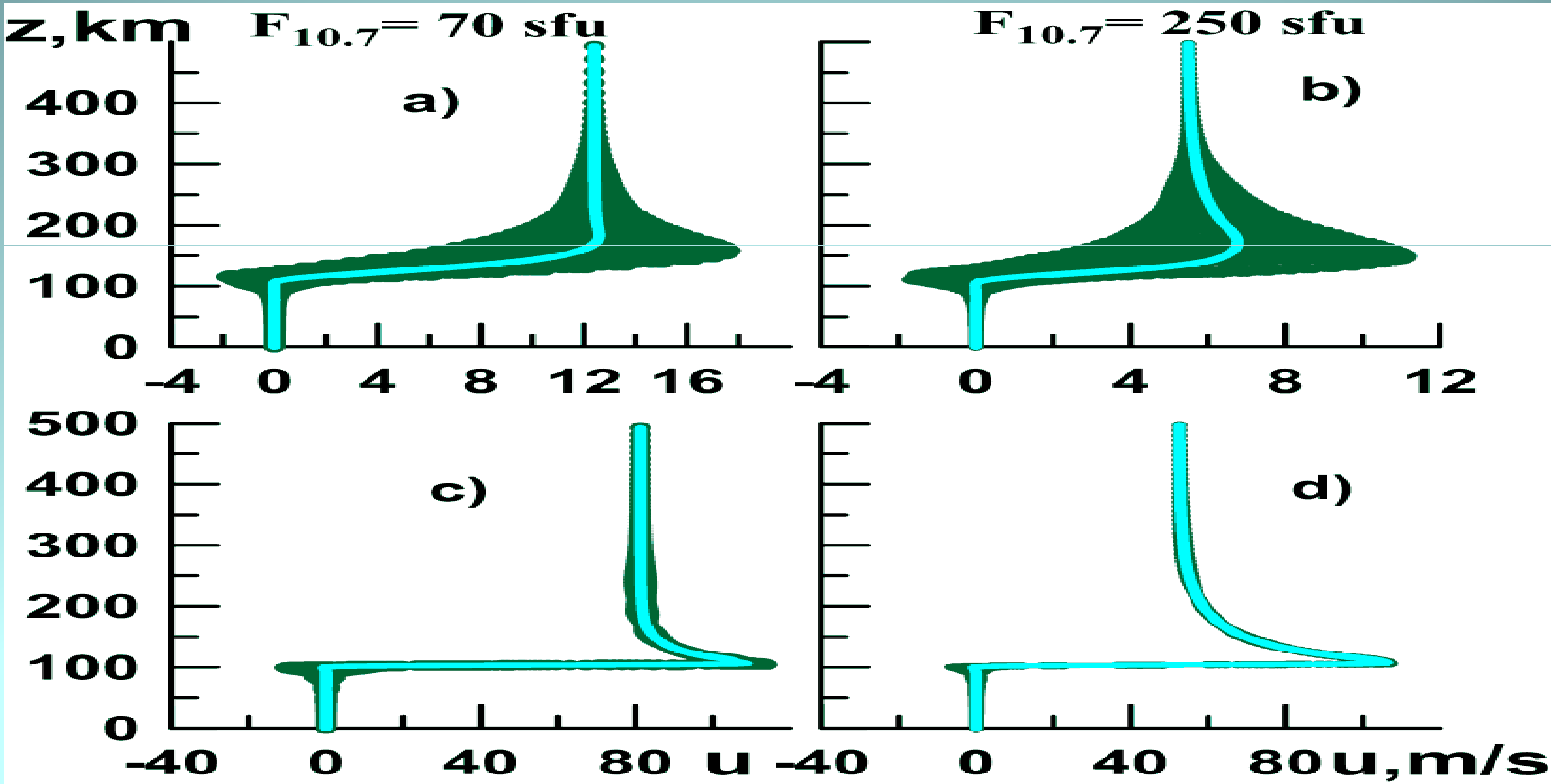

Time variations of vertical wave flux of horizontal momentum

at altitudes 250 (a), 200 (b), 150 (c), 120 (d), 110 km (e) for amplitudes W_0 = 0.1 mm/s (left) and W_0 = 1 mm/s (right) of the surface wave forcing with period $\tau = 2 \cdot 10^3$ s and c_x = 100 m/s at low (blue) and high (red) levels of solar activity

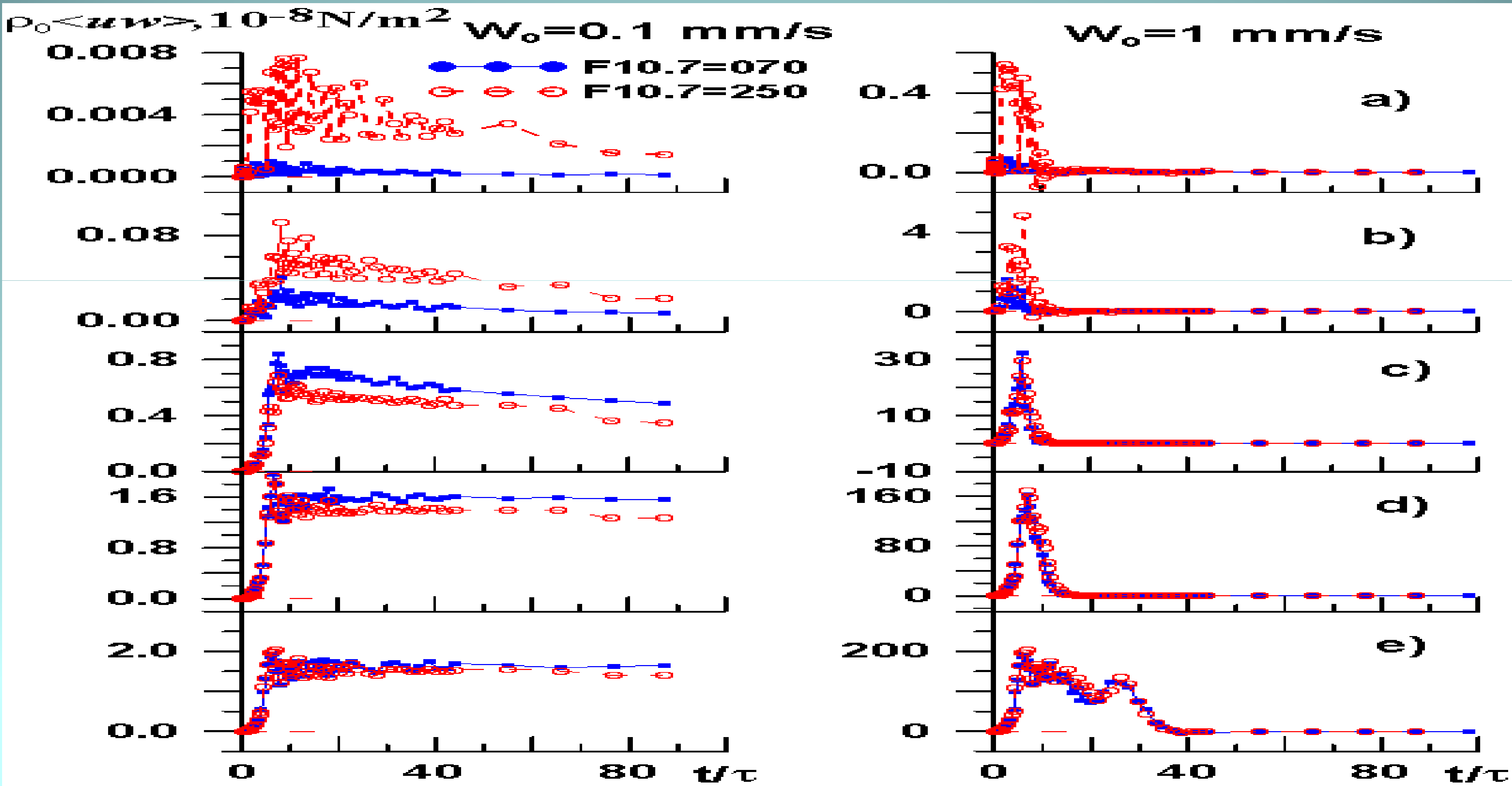

Time variations of wave accelerations of the mean flow

at altitudes 250 (a), 200 (b), 150 (c), 120 (d), 110 km (e) for amplitudes W_0 = 0.1 mm/s (left) and W_0 = 1 mm/s (right) of the surface wave forcing with period $\tau = 2{\cdot}10^3$ s and c_x = 100 m/s at low (left) and high (right) levels of solar activity.

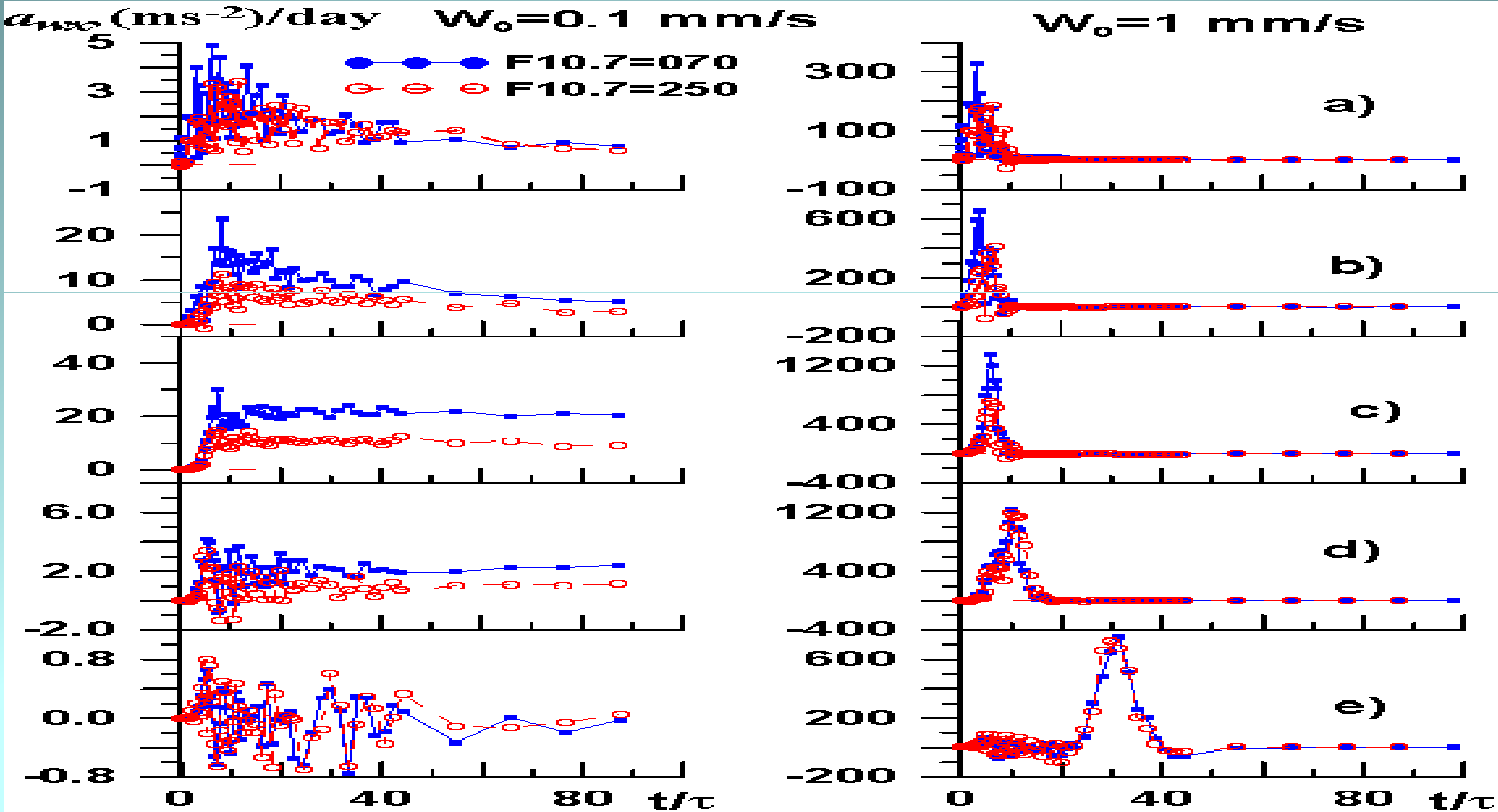

Time variations of the mean horizontal velocity

at altitudes 250 (a), 200 (b), 150 (c), 120 (d), 110 km (e) for amplitudes W_0 = 0.1 mm/s (left) and W_0 = 1 mm/s (right) of the surface wave forcing (1) with period $\tau = 2 \cdot 10^3$ s and c_x = 100 m/s at low (blue) and high (red) levels of solar activity.

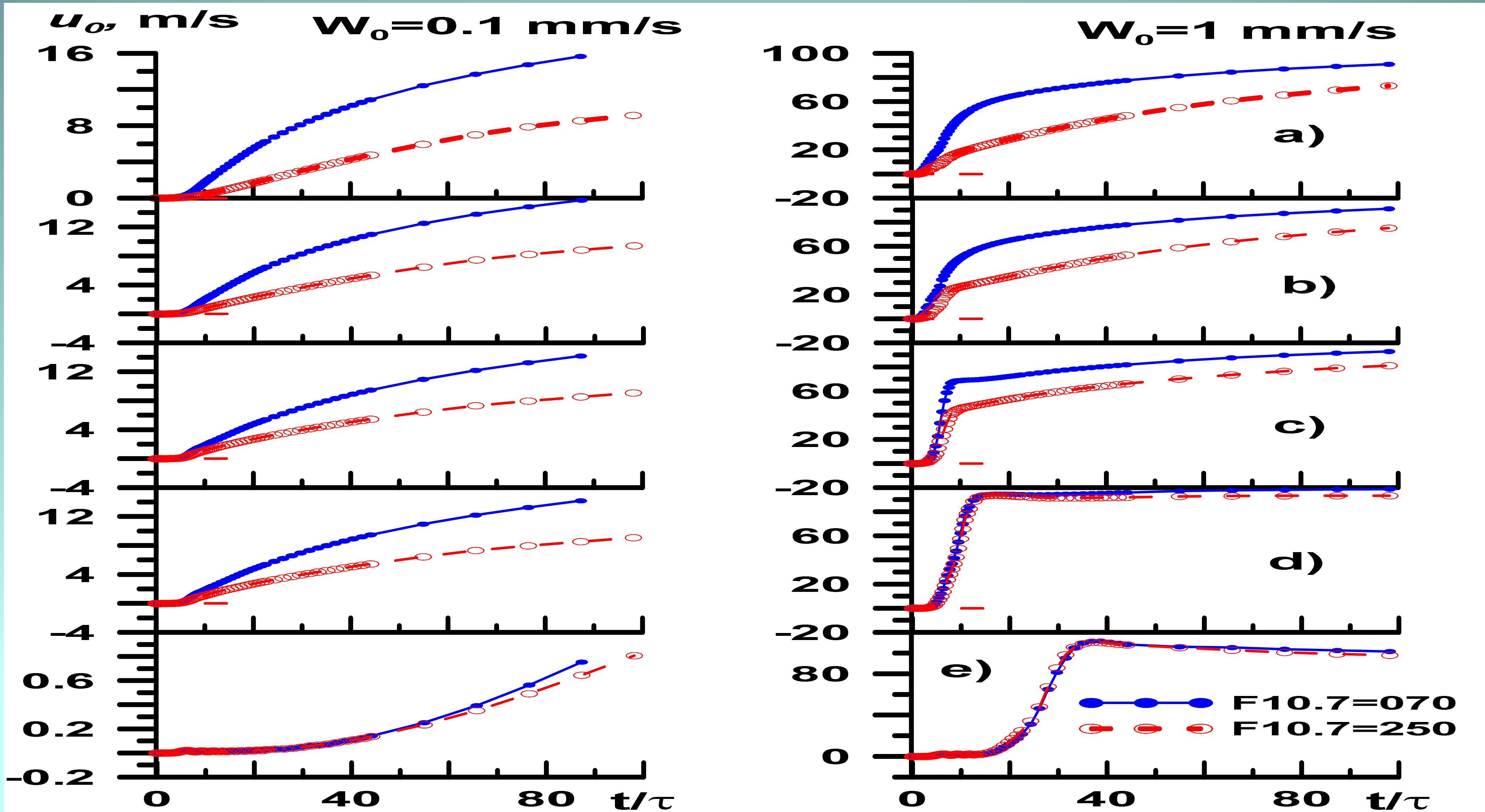

Time variations of the mean vertical velocity

at altitudes 250 (a), 200 (b), 150 (c), 120 (d), 110 km (e) for amplitudes $W_0 = 0.1$ mm/s (left) and $W_0 = 1$ mm/s (right) of the surface wave forcing with period $\tau = 2 \cdot 10^3$ s and $c_x = 100$ m/s at low (blue) and high (red) levels of solar activity.

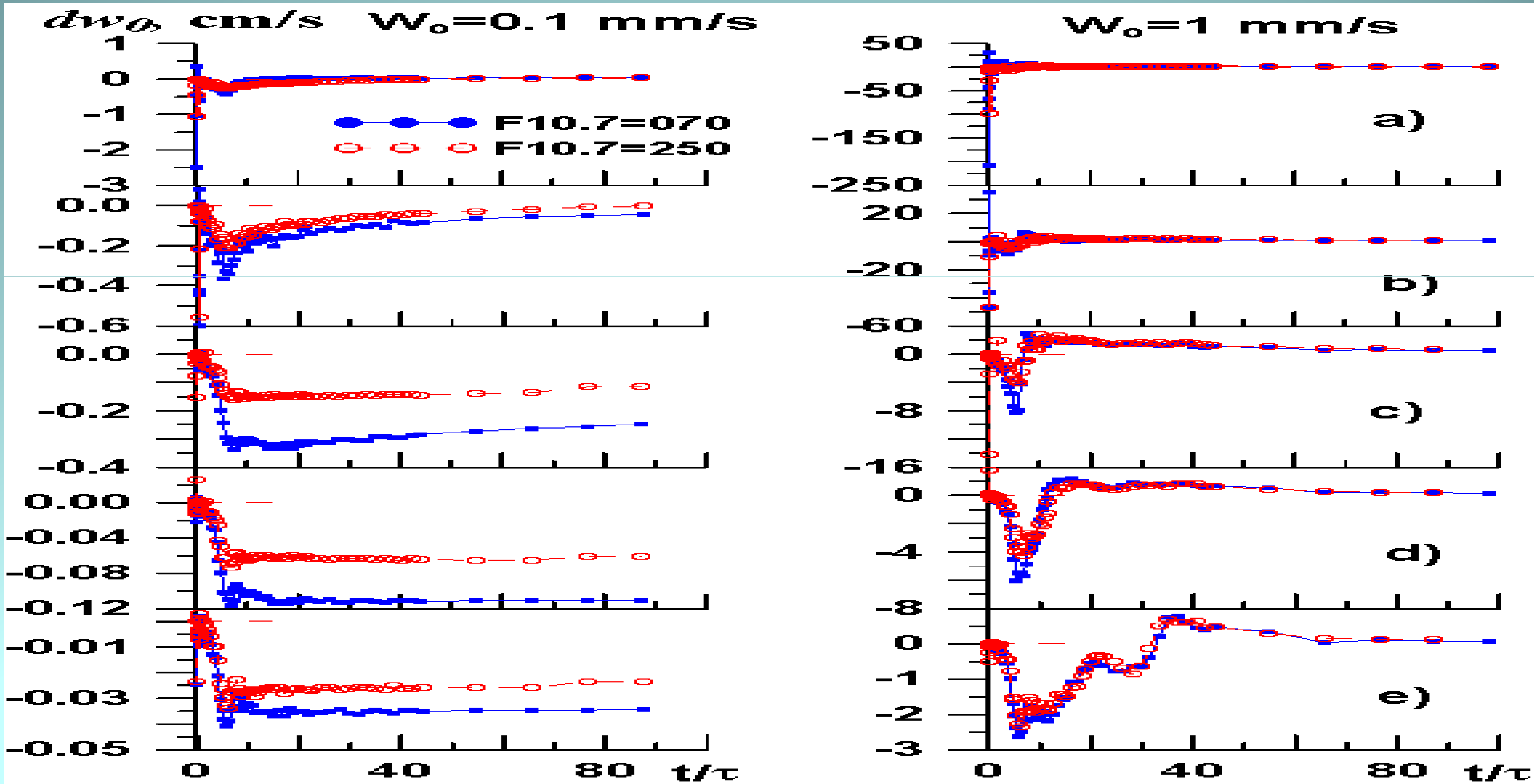

6. AGW thermal effect

Time variations of the mean temperature

at altitudes 250 (a), 200 (b), 150 (c), 120 (d), 110 km (e) for amplitudes W_0 = 0.1 mm/s (left) and W_0 = 1 mm/s (right) of the surface wave forcing (1) with period τ = $2{\cdot}10^3$ s and c_x = 100 m/s at low (blue) and high (red) levels of solar activity.

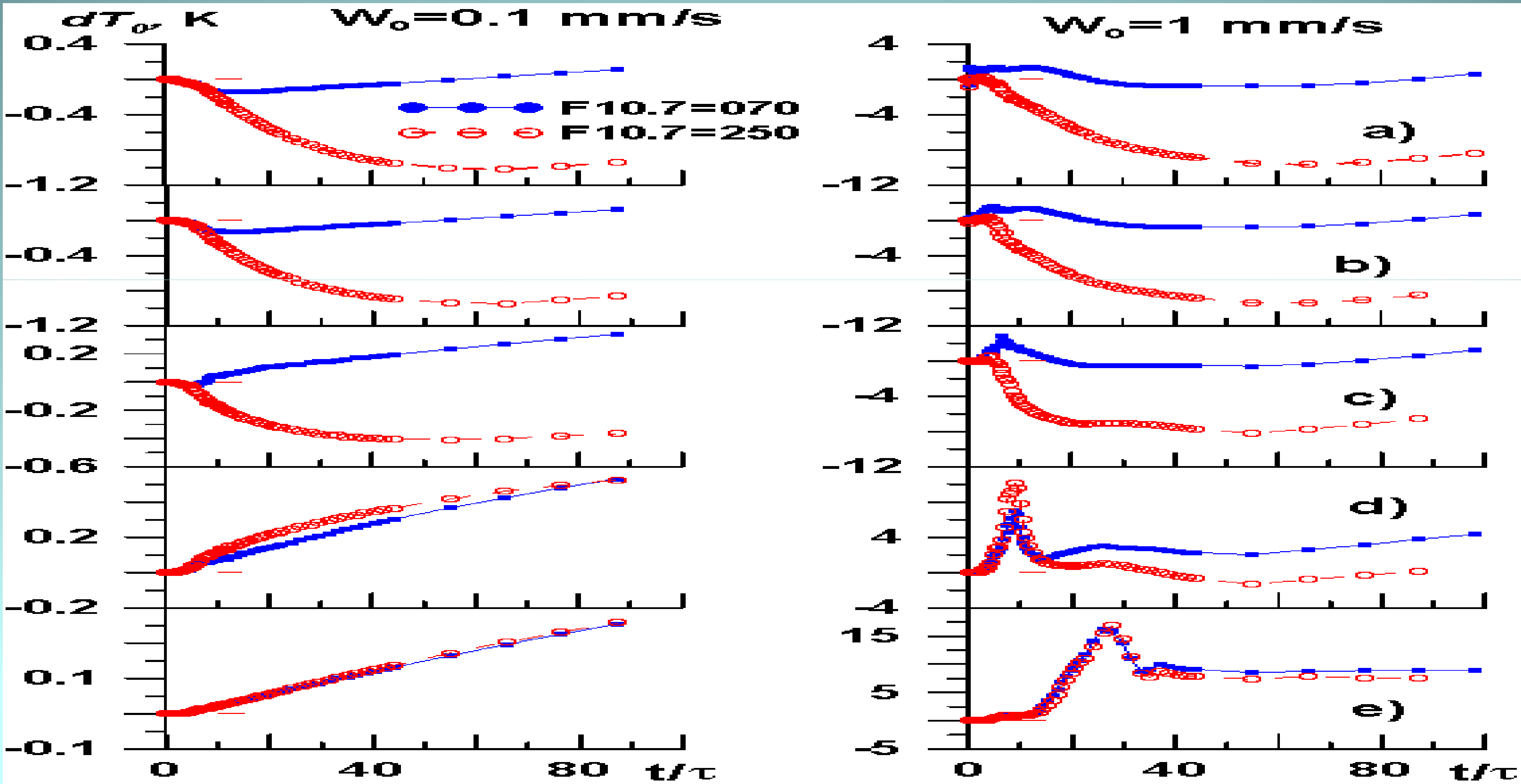

Time variations of the wave heat flux

at altitudes 250 (a), 200 (b), 150 (c), 120 (d), 110 km (e) for amplitudes W_0 = 0.1 mm/s (left) and W_0 = 1 mm/s (right) of the surface wave forcing (1) with period $\tau = 2{\cdot}10^3$ s and c_x = 100 m/s at low (blue) and high (red) levels of solar activity.

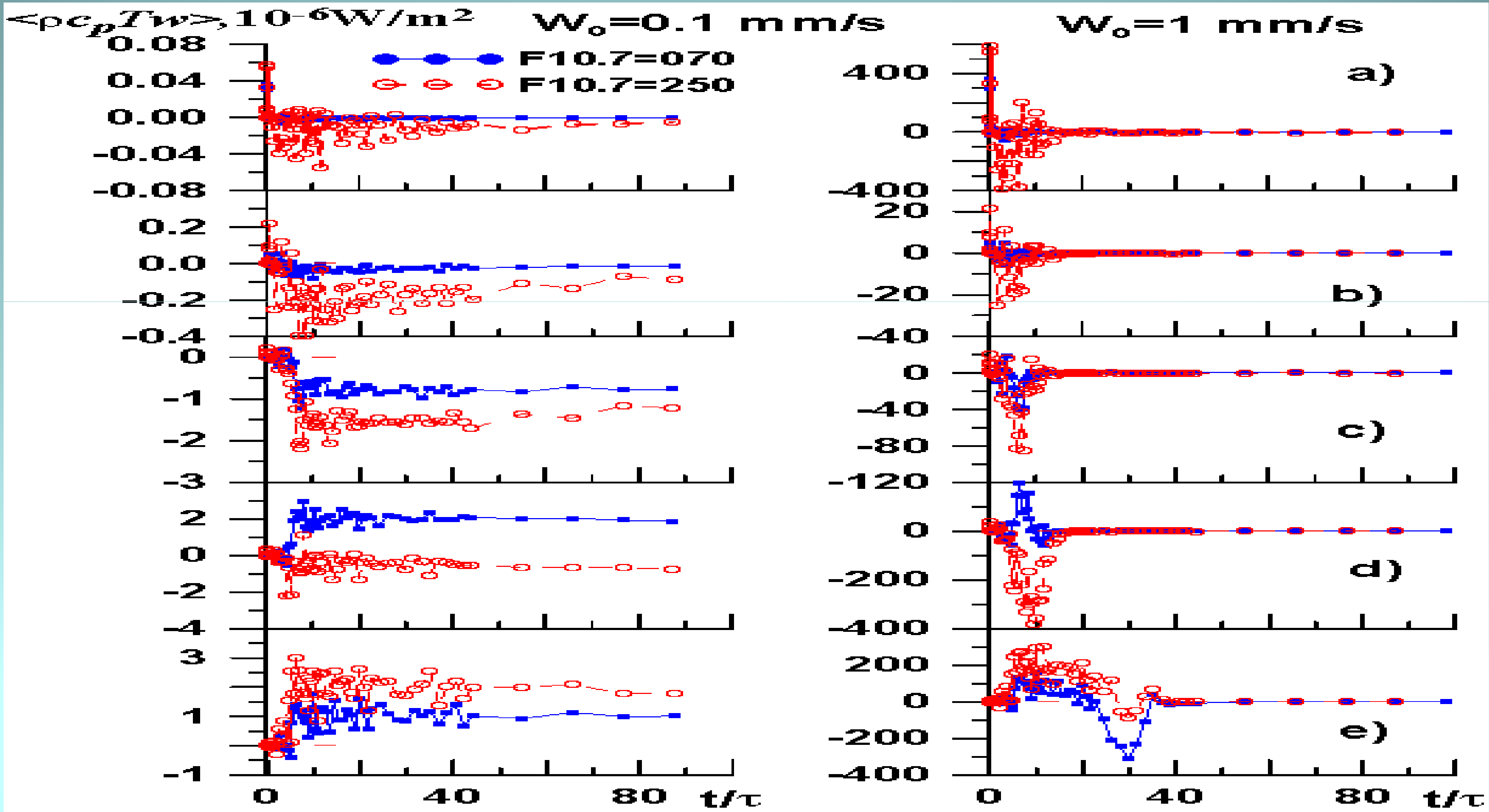

Time variations of the wave energy flux

at altitudes 250 (a), 200 (b), 150 (c), 120 (d), 110 km (e) for amplitudes W_0 = 0.1 mm/s (left) and W_0 = 1 mm/s (right) of the surface wave forcing with period τ = $2 \cdot 10^3$ s and c_x = 100 m/s at low (blue) and high (red) levels of solar activity.

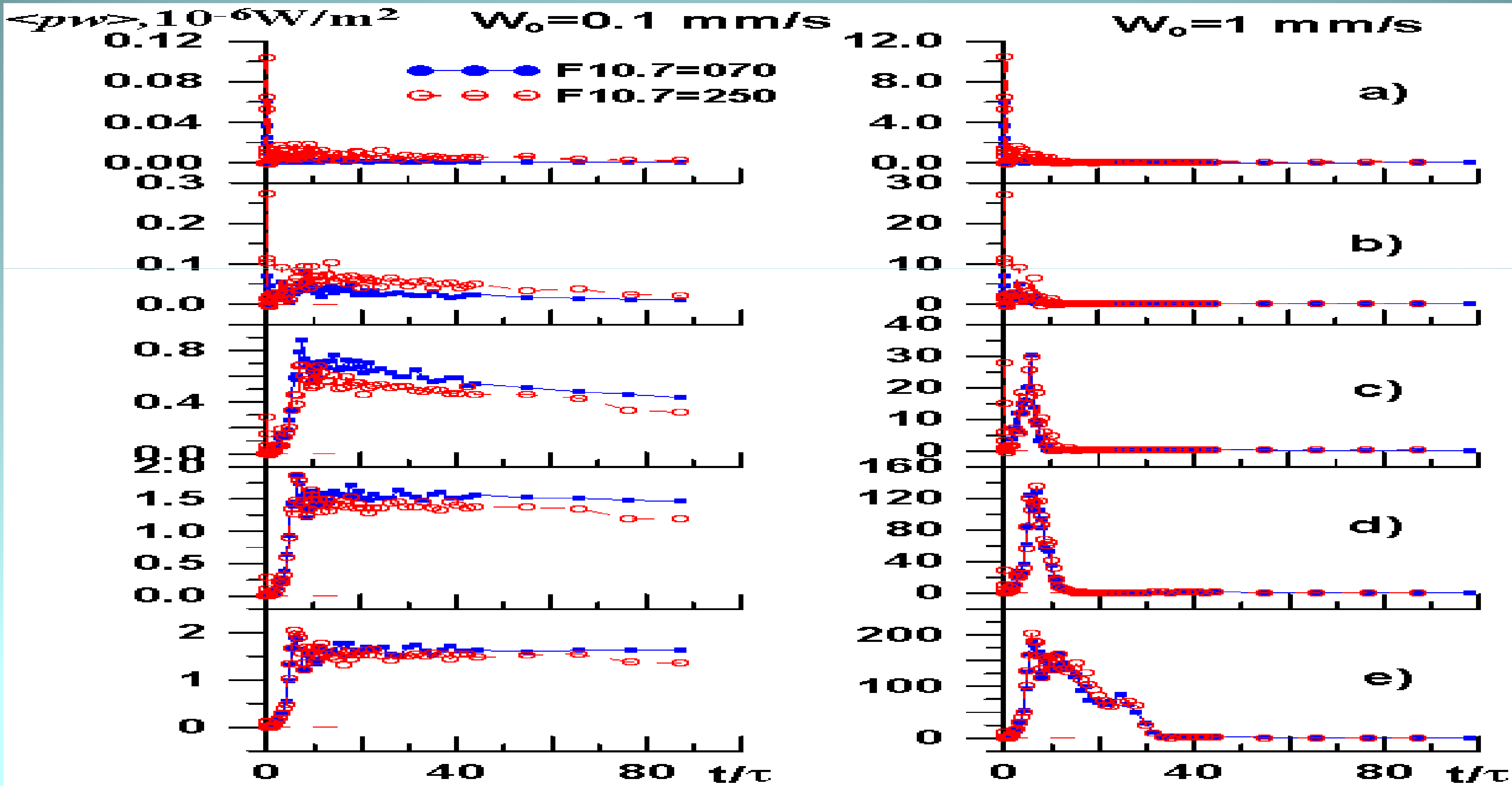

Time variations of the wave mass flux

at altitudes 250 (a), 200 (b), 150 (c), 120 (d), 110 km (e) for amplitudes W_0 = 0.1 mm/s (left) and W_0 = 1 mm/s (right) of the surface wave forcing with period $\tau = 2 \cdot 10^3$ s and c_x = 100 m/s at low (blue) and high (red) levels of solar activity.

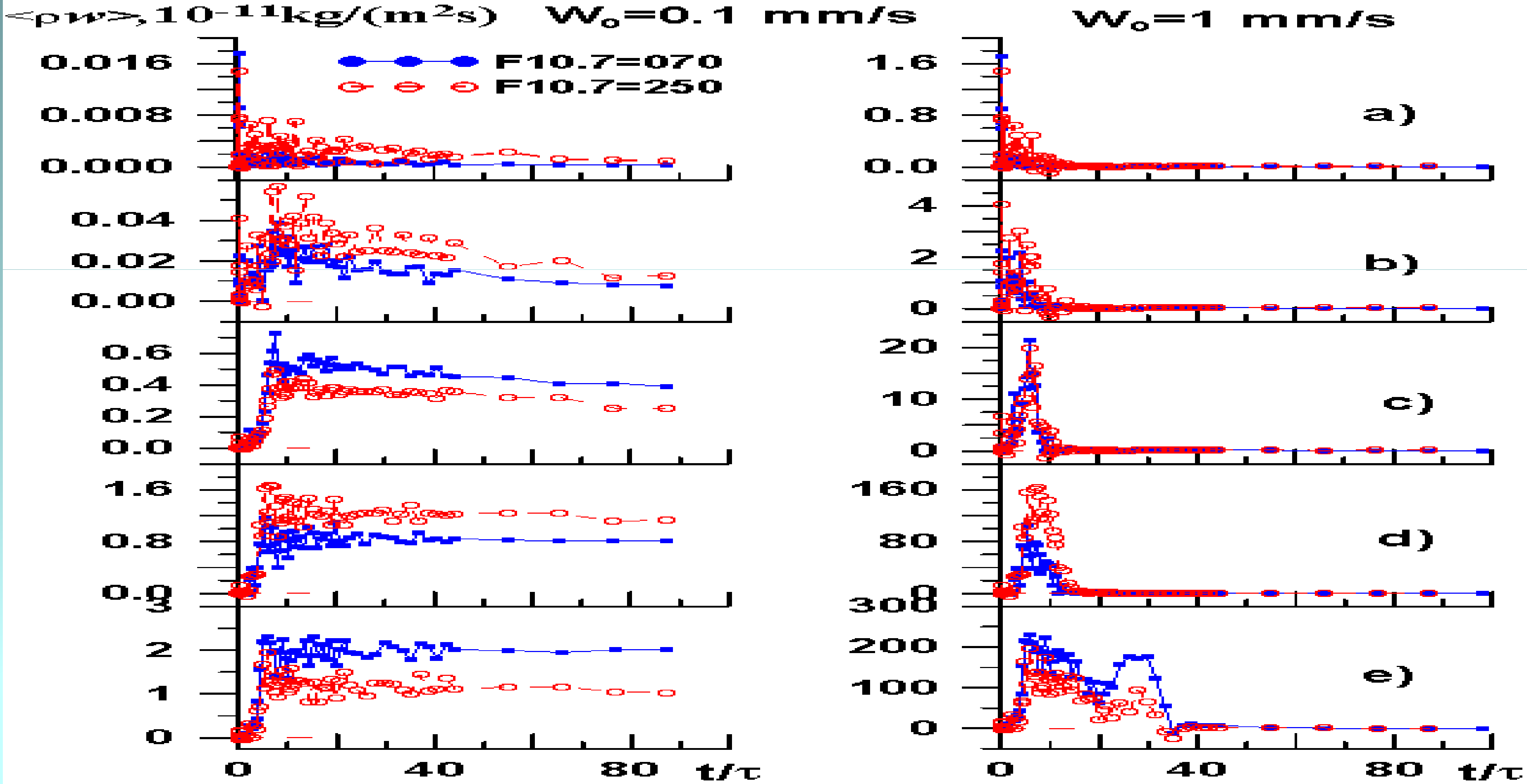

Conclusion

1. Change in background temperature, density and molecular viscosity due to solar activity influences AGW characteristics, wave-induced jets and wave heating of the upper atmosphere.

2. Wave accelerations and wave-induced jet streams are larger at lower solar activity.

3. Above altitudes 150 km, IGWs produce heating at low solar activity and cooling at high solar activity.

4. Numerical simulation of nonlinear AGW propagation helps better underst anding the details of dynamical and thermal influence of waves coming from the troposphere on the mean temperature and wind in the middle and upper atmosphere.